


 Cite this: *RSC Adv.*, 2020, 10, 19832

# A stimuli-responsive, superporous and non-toxic smart hydrogel from seeds of mugwort (*Artemisia vulgaris*): stimuli responsive swelling/deswelling, intelligent drug delivery and enhanced aceclofenac bioavailability†

 Muhammad Farid-ul-Haq,<sup>a</sup> Muhammad Ajaz Hussain,<sup>ID</sup> \*<sup>a</sup>  
 Muhammad Tahir Haseeb,<sup>b</sup> Muhammad Umer Ashraf,<sup>c</sup> Syed Zajif Hussain,<sup>ID</sup> <sup>d</sup>  
 Tahira Tabassum,<sup>e</sup> Irshad Hussain,<sup>ID</sup> <sup>d</sup> Muhammad Sher,<sup>a</sup>  
 Syed Nasir Abbas Bukhari<sup>ID</sup> <sup>f</sup> and Muhammad Naeem-ul-Hassan<sup>ID</sup> <sup>a</sup>

*Artemisia vulgaris* seeds extrude hydrogel (AVH), which shows extraordinary swelling in water, at pH 6.8, and 7.4, which follows second-order kinetics. AVH exhibits reversible swelling/deswelling in ethanol and normal saline as well at pH 7.4 and pH 1.2. Therefore, AVH shows stimuli-responsiveness in different physiological conditions, solvents, and electrolytes. The superporous nature of AVH in swollen/freeze-dried sculpture is exposed in their SEM micrographs. AVH-based aceclofenac tablet formulations offer sustained-release under simulated conditions of the gastrointestinal tract (GIT) in terms of pH and transit time. Pharmacokinetic studies also show the delay and prolonged plasma concentration with  $t_{\max}$  of 8 h, therefore, such formulations can be used to enhance the bioavailability of aceclofenac. The swelling behavior of the AVH tablet is also assessed using MRI. The *in vivo* fate of the AVH tablet is monitored by X-ray during the transit through the GIT. Acute toxicity studies of AVH indicate the absence of any toxicity which reveals the safety profile of AVH. Therefore, AVH can be used for oral, topical and ophthalmic drug delivery systems. These results establish the potential of AVH as a stimuli sensitive, pH-dependent, and sustained-release biomaterial for targeted drug delivery.

Received 8th April 2020

Accepted 18th May 2020

DOI: 10.1039/d0ra03176c

[rsc.li/rsc-advances](http://rsc.li/rsc-advances)

## 1 Introduction

From the ancient era, plants played a vital role in human daily life from functional food to medicine.<sup>1,2</sup> Besides that, seed coats of several plants extrude mucilage on coming in contact with water.<sup>3–5</sup> This mucilage consists of polysaccharides that swell extraordinarily in water. Such materials are smart/intelligent as they offer on–off swelling behavior *vs.* various external stimuli like pH, electrolyte stress, solvents, and temperature, *etc.* Due to their

superporous nature, pH-responsiveness, on–off switching behavior, such naturally occurring water-swellaable and pH-sensitive functional materials are in high demand to develop sustained/controlled/targeted oral tablet formulations in design and drug delivery.<sup>6,7</sup> Such smart natural polysaccharides also gaining the attention of researchers due to their diverse functionalities, biocompatibility, biodegradability, bio-adhesiveness, and non-immunogenic nature.<sup>8</sup> These innate properties in such natural polysaccharides lead to the development of several advanced drug delivery systems like microgels, nanogels and hydrogels,<sup>9,10</sup> and pH-sensitive, mucoadhesive and sustained-release oral formulations.<sup>2,11</sup> Drug release from a swellaable/hydrogelable polymeric material mainly depends upon the swelling capacity of the material, pH/nature of the media, and the possible interaction between polymer and the drug. Therefore, the determination of the swelling capacity is very important for the development of stimuli-responsive sustained release formulation. As the drug release is dependent on the swelling of the polysaccharides and their pH-responsiveness, therefore, the extent and rate of drug release from such polysaccharides can be controlled or modified by adding the suitable concentration of these materials to develop highly precise drug delivery system.<sup>7,12</sup>

<sup>a</sup>Department of Chemistry, University of Sargodha, Sargodha 40100, Pakistan. E-mail: majaz172@yahoo.com

<sup>b</sup>College of Pharmacy, University of Sargodha, Sargodha 40100, Pakistan

<sup>c</sup>Department of Pharmaceutics, Faculty of Pharmacy, The University of Lahore, Lahore 54000, Pakistan

<sup>d</sup>Department of Chemistry, SBA School of Science & Engineering, Lahore University of Management Sciences, Lahore Cantt. 54792, Pakistan

<sup>e</sup>Faculty of Medical and Health Sciences, Sargodha Medical College, University of Sargodha, Sargodha 40100, Pakistan

<sup>f</sup>Department of Pharmaceutical Chemistry, College of Pharmacy, Jouf University, 2014, Sakaka, Aljouf, Saudi Arabia

† Electronic supplementary information (ESI) available. See DOI: 10.1039/d0ra03176c



We are interested to introduce a novel smart hydrogel from seeds of *Artemisia vulgaris* (AVH) and to evaluate its swelling potential and swelling/deswelling properties in different physiological pH and various media. Herein, we are also reporting the appraisal of sustained/controlled drug release potential of AVH-based tablet formulations in simulated gastric fluid (SGF) and simulated intestinal fluid (SIF). Aims are to evaluate the swelling behavior/mechanism of an AVH-based tablet formulation *in vitro* using MRI. The GIT transit of the AVH-based tablet formulation will be evaluated *in vivo* in stray dogs using radiography and performed the pharmacokinetic studies to sketch the bioavailability of aceclofenac from AVH-based intelligent drug delivery system. Acute toxicity studies of AVH and histological evaluation are also aimed to establish the non-toxic nature of this novel and smart material.

## 2 Materials and methods

### 2.1 Materials

*Artemisia vulgaris* (AV) seeds were procured from Seed Needs, LLC. Ethanol, KCl, NaCl, NaOH, HCl, *n*-hexane and potassium dihydrogen phosphate ( $\text{KH}_2\text{PO}_4$ ) were procured from Riedel-de Haën, Germany. Magnesium stearate was acquired from BDH (Bristol, England). Microcrystalline cellulose was purchased from Merck, Germany. Tragacanth gum was obtained from Sigma-Aldrich, USA. Aceclofenac was of European Pharmacopoeia (EP) standard. Preparation of simulated gastric fluid (SGF) and simulated intestinal fluid (SIF) were accomplished as described in United States Pharmacopoeia (USP). Water used throughout the study was deionized.

### 2.2 Isolation of AV hydrogel

AV seeds (100 g) were cleaned to remove filthy material and soaked in deionized water (800 mL) for 24 h. Soaked seeds were then heated at 60 °C for 0.5 h before the extrusion of mucilage. AV hydrogel (AVH) was separated from seed coats by placing them in a nylon mesh and gentle rubbing. AVH was washed with deionized water followed by *n*-hexane to remove wax or lipophilic substances. AVH was vacuum dried at 60 °C for 48 h then milled and passed through mesh no. 60 before storage in a desiccator. The yield of AVH was 13.68 wt%.

### 2.3 Characterization of AVH

AVH was characterized through Fourier transform infrared (FTIR) spectroscopy, thermogravimetric analysis (TGA), energy-dispersive X-ray spectroscopy (EDX) and solid-state CP/MAS  $^{13}\text{C}$  NMR spectroscopy to confirm the polysaccharide nature of the isolated hydrogel. FTIR spectroscopy was performed on IR prestige-21 (Shimadzu, Japan) using the pellet method in which AVH was mixed with KBr and then compressed under hydraulic pressure to make a thin pellet. Before recording the FTIR spectrum, the pellet was dried at 50 °C for 1 h each time. Spectra were then recorded in the range from 4000–400  $\text{cm}^{-1}$ .

Thermal stability and decomposition temperatures of AVH were analyzed using SDT Q600 thermal analyzer (TA Instruments, USA). TGA was recorded from ambient to 800 °C at the onset of

10 °C  $\text{min}^{-1}$  under nitrogen. Thermal decomposition data was processed through Universal Analysis 2000 v 4.2E software.

The porosity of interconnected channels having micropores in AVH and tablet was resolute with a scanning electron microscope (FEI-NOVA, NanoSEM-450) operative at 10 kV and a working distance of 5 mm 10 kV. In parallel, its elemental-composition was analyzed using energy-dispersive X-ray spectroscopy (EDS) *via* Oxford-EDS detector fitted with this SEM operating under the same conditions.

Solid-state CP/MAS  $^{13}\text{C}$  NMR spectrum of AVH was recorded on a Bruker DRX-400 (100 MHz) machine at ambient temperature (proton 90°, acquisition time 0.032 s, pulse time 4.85  $\mu\text{s}$ , delay time 2 s) spectrum of AVH was acquired at ambient temperature.

### 2.4 Dynamic and equilibrium swelling of AVH

To probe dynamic swelling behavior and water holding capacity of AVH, pH 1.2, 4.5, 6.8 and 7.4 buffers, and water were employed using widely accepted tea bag method.<sup>13–15</sup> To ascertain the effect of temperature on the swelling capacity of AVH, swelling studies were also carried out at 25, 37 and 50 °C in deionized water. In a typical procedure, AVH (0.1 g) was taken in a pre-weighed cellophane tea bag and immersed in the buffer of pH 1.2. Periodically, tea bag was taken out of the buffer and weighed after blotting or removing excess solution. The swelling capacity of AVH was calculated using eqn (1).

$$\text{Swelling capacity (g g}^{-1}\text{)} = \frac{W_t - W_0 - W_c}{W_0} \quad (1)$$

where,  $W_0$  is the weight of the dry AVH,  $W_t$  denotes the weight of the swollen AVH along with the wet cellophane tea bag and  $W_c$  represents the weight of the wet cellophane tea bag.

After calculating swelling capacity, tea bag was again placed in the buffer for a predefined time interval for further readings up to 12 h. The same procedure of swelling capacity of AVH was performed in pH 6.8 and 7.4, and water. The maximum swelling capacity of AVH was also recorded by a similar method but up to 24 h. Each experiment was executed six times and mean values are reported.

The normalized degree of swelling ( $Q_t$ ) at any time  $t$  is the ratio of the amount of water retained by AVH to its dry weight and calculated using eqn (2).<sup>16</sup>

$$Q_t = \frac{W_s - W_d}{W_d} = \frac{W_t}{W_d} \quad (2)$$

where,  $W_t$  indicates the weight of water trapped into the hydrogel at time  $t$ ,  $W_s$  indicates the weight of swollen hydrogel at time  $t$  and  $W_d$  shows the weight of dried hydrogel at time  $t = 0$ .

The  $Q_e$  represents the normalized equilibrium degree of swelling that is the ratio of the weight of swelling media retained by AVH at  $t = \infty$  (time required to attain maximum swelling) to the weight of AVH at  $t = 0$ . It is calculated using eqn (3).

$$Q_e = \frac{W_\infty - W_d}{W_d} = \frac{W_e}{W_d} \quad (3)$$

where,  $W_\infty$  indicates the weight of swollen AVH at time  $t_\infty$ ,  $W_d$  denotes the weight of dried AVH at  $t = 0$ , and  $W_e$  is the quantity of water penetrate in the AVH matrix at time  $t = \infty$ .



## 2.5 Swelling kinetics of AVH

Swelling kinetics of AVH was evaluated from  $Q_t$  and  $Q_e$  to determine the rate of absorbency of the swelling media. A straight-line graph between  $t/Q_t$  on  $y$ -axis and  $t$  on the  $x$ -axis represents second-order swelling kinetics (eqn (4)) having a slope of  $1/Q_e$  and an intercept of  $1/KQ_e^2$ .<sup>17</sup>

$$\frac{t}{Q_t} = \frac{1}{KQ_e^2} + \frac{t}{Q_e} \quad (4)$$

## 2.6 Saline responsive swelling of AVH

To appraise the effect of electrolytes and their concentration on the swelling capacity of AVH, aq. solution of 0.01, 0.03, 0.05, 0.07, 0.09, 0.1, 0.3, 0.5, 1.0, 1.5 and 2.0 M KCl and NaCl were used. The swelling was recorded for 24 h using tea bag method as described earlier.

## 2.7 Swelling/deswelling (on-off switching) behavior of AVH

Swelling/deswelling capabilities of AVH were evaluated in swelling media (deionized water and buffer solution of pH 7.4) and then shifted to deswelling media (ethanol, normal saline and buffer solutions of pH 1.2). Both swelling and deswelling phases of AVH was carried out for 1 h. During each phase, after regular and predetermined time intervals, the swelling capacity of AVH was determined as described earlier. Each experiment was performed six times and mean values are reported. A similar approach was adopted for swelling/deswelling of AVH in deionized water and normal saline, and deionized water and ethanol.

## 2.8 Scanning electron microscopy

To observe porosity/channeling in AVH and AVH-based tablets, the SEM technique was used. AVH (0.1 g) was mixed in Milli-Q water (2 mL) using mill-mixer and sonicated. Separately, the tablet was dipped in water for 24 h to get swollen. Then both, mixtures of the above prepared AVH and swollen tablet, were freeze-dried. Subsequently, the freeze-dried AVH was subjected to cut into its longitudinal and vertical cross-sections with a sharp knife; and then the prepared samples of AVH and tablet were fixed onto a multipoint SEM aluminum-stub before gold coating with Denton-Desk V-HP sputter coater operated under vacuum at 40 mA for 30 s.

## 2.9 Preparation of tablets

Aceclofenac (ACF) was selected to evaluate its sustained-release potential from AVH-based oral tablet formulations using the wet granulation method (Table S1, ESI†). AVH, ACF and microcrystalline cellulose were mixed and homogenized by trituration followed by moistened with aq. solution of tragacanth gum (5% w/v). Damp mass was converted into granules by passing through sieve no. 12, dried at 40 °C for 8 h, pass through sieve no. 20 and lubricated with magnesium stearate. These granules were evaluated through pre-compression parameters, *i.e.*, angle of repose, Hausner ratio and Carr's index, and values were calculated as 30.7, 1.16 and 14.9%,

respectively. According to United States Pharmacopeia 35, these values are recognized as "good" values. Lubricated granules were subjected to compression on a rotary press equipped with an 11 mm flat surface punch. Each tablet was compressed at a weight, hardness and thickness of 400 mg ± 10 mg, 7–8 kg cm<sup>-2</sup> and 3.90–4.00 mm, respectively.

## 2.10 In vitro drug release studies

To explore the effect of AVH concentration on *in vitro* ACF release, three different formulations (ACF1, ACF2, and ACF3) with varying concentrations of AVH were designed (Table S1, ESI†). The dissolution studies were performed in each of simulated gastric fluid (SGF) and simulated intestinal fluid (SIF) for 12 h at 37 °C ± 0.5 °C. Additionally, mimicking the GIT conditions (pH and transit time), the dissolution studies were also performed in SGF (900 mL) for 2 h and SIF (900 mL) up to 10 h in USP dissolution apparatus II (50 rpm). Aliquots of dissolution medium (4 mL) were taken out at predetermined time intervals, filtered, suitably diluted and analyzed on a UV-visible spectrophotometer (Shimadzu, Japan) at 280 nm. All dissolution studies were performed in triplicate. To understand the underlying mechanism of drug release from the polymer matrix, drug release data were evaluated using the power-law eqn (5).<sup>18,19</sup>

$$\frac{M_t}{M_\infty} = k_p t^n \quad (5)$$

where,  $M_t/M_\infty$  indicates the fraction of drug released at time  $t$ ,  $n$  is the diffusion coefficient and  $k_p$  is power-law constant.

## 2.11 Pharmacokinetic studies

Pharmacokinetic profile of the developed formulation was performed in healthy stray dogs (18–20 kg). Animals were kept in the laboratory under light and dark cycles (12 h each) in clean cages one week before the start of experiments to acclimatize the laboratory conditions. During this period, a standard laboratory diet and ordinary tap water were provided to the animals. Six dogs were selected and divided into two groups. The experimental procedure was approved by the Institutional Research Ethics Committee of The University of Lahore, Lahore vide letter no. IREC-2018-76-M on May 17, 2018.

For pharmacokinetic studies, formulation ACF1 was administered to overnight fasted animals of sample group whereas the control group was given the aqueous suspension of aceclofenac (100 mg/10 mL). After periodic time intervals (0, 0.5, 1, 1.5, 2, 3, 4, 6, 8, 10, 12, 16 and 24 h), blood sample was collected in heparinized tubes. Plasma was separated through centrifugation and determined the concentration of aceclofenac through the reported HPLC method.<sup>20</sup> Different pharmacokinetic parameters were calculated from the plasma concentration–time curve.

## 2.12 Stimuli-responsive swelling study of tablet formulations

The swelling behavior of tablets (ACF1, ACF2, and ACF3) was observed at pH 7.4 following the procedure and eqn (5) as



described earlier. Stimuli-responsive swelling/deswelling of formulation ACF1 was performed at pH 7.4 and 1.2, deionized water and normal saline, and deionized water and ethanol as described earlier for AVH. During swelling studies of tablets, photographs were taken after regular intervals to observe the shape of swollen tablets.

### 2.13 *In vivo* X-ray study

A tablet containing AVH and barium sulfate (radio opaquant) was prepared following the wet granulation method. The composition of AVH tablet for X-ray study (formulation AVHF) was the same as of ACF3 except ACF was replaced with BaSO<sub>4</sub> (Table S1, ESI†).<sup>21</sup> It was observed that pre- and post-compression parameters of formulations AVHF and ACF3 were comparable which was essential to maintain the similarities between two formulations. For *in vivo* X-ray study, healthy stray dogs (16–18 kg) were selected.<sup>22</sup> All animals were acclimatized to laboratory conditions for one week. Furthermore, animals were kept fast overnight before the day of the experiment. AVHF tablet was administered to a stray dog through a gavage tube followed by ordinary tap water (100 mL). Animals were given free access to water whereas refrained from food for 8 h. The emptiness of the stomach from any opaquant was verified by taking an X-ray image, then after ingestion of tablet, radiographs of GIT were taken after regular intervals to observe the transit of the tablet in GIT. The X-ray machine (Beam Limiting Device, Model TF-6TL-6, Toshiba Corporation, Japan) was operated at a voltage and current intensity of 70 kV and 400 mA s, respectively. The study protocols/procedures were approved by the Institutional Research Ethics Committee of The University of Lahore, Lahore vide letter no. IREC-2018-76-M on May 17, 2018, and are per the directions of the National Institute of Health's Guidelines for the Care and Use of Laboratory Animals (NIH Publications No. 8023, revised 1978).

### 2.14 Swelling/erosion studies of AVH tablet by MRI

*In situ* swelling and erosion behavior of AVH tablet formulation (AVHM) was observed through MRI (Siemens Concerto Open MRI, Germany) equipped with a superconducting magnet having a magnetic field strength of 0.25 T. MRI detects the <sup>1</sup>H which is associated with free water. Additionally, signal intensity also relates to the T<sub>2</sub> (spin–spin relaxation) and T<sub>1</sub> (spin-lattice relaxation) values.<sup>23</sup> Formulation AVHM was prepared from AVH (250 mg), tragacanth gum (40 mg) and magnesium stearate (5 mg) using wet granulation method. For the MRI experiment, AVHM tablets were placed in a buffer of pH 1.2 and 7.4 and in deionized water maintained at 37 ± 0.5 °C for swelling up to 8 h. The magnetic stirring of the tablet in media was avoided in MRI experiments. Images were captured at regular intervals in black and white mode and interpreted using a computer program (Syngo 2004A).

### 2.15 Acute toxicity studies model and procedure

Acute toxicity studies of AVH were carried out on Swiss albino rats (150–200 g). For acute dermal toxicity and eye irritation test, Swiss albino rabbits (1400–1500 g) were selected. Animals of either sex were obtained from the animal house of the University of

Sargodha, Sargodha and were examined for sickness and anomalies and shifted to the laboratory where they were divided in to five groups (5 animals in each group) and shifted to neat and clean cages. All animals were kept at 25 °C and 40% humidity. Animals (mice) were given free access to diet and tap water. All animals were fed with standard pellet diet. All tests were conducted by complying the good laboratory practices (GLP) as described by the United States Food and Drug Administration (USFDA). In current acute toxicity studies, all the procedures adopted complied with the regulations of the Organization for Economic Co-operation and Development (OECD). The protocol of the study was approved by the Pharmacy Research Ethics Committee of the University of Sargodha, Sargodha, Pakistan.

Acute oral toxicity studies were conducted as per the guidelines of OECD for analysis of toxicity induced by chemicals. Animals of sample group (Group II, III and IV) were treated with a single dose of AVH (50, 300 and 2000 mg kg<sup>-1</sup>), respectively, mixed with standard food whereas, control group (Group I) was administered only standard food (Table S2, ESI†).

After the administration of AVH, animals were monitored closely for the allergic reaction, diarrhea, reflexes, salivation, tremors for 8 h and daily over 14 days. Additionally, bodyweight of the animals and food and water consumption were also recorded. After 14 days, all vital organs such as kidney, heart, spleen, lungs, liver and gastrointestinal tract (GIT) were removed and examined macroscopically for lesions. The absolute organ weight of each organ of both control and test animals were recorded.

For eye irritation and acute dermal toxicity, five albino rabbits were thoroughly examined for eye lesions according to the Draize scale.<sup>24</sup> AVH suspension in deionized water (5 mg/10 mL) was prepared and instilled into the conjunctival sac of the right eye of each rabbit. Eyes were examined after 1, 2, 4, 24, 48 and 72 h for redness, allergic symptoms, swelling, lacrimation, and corneal opacity. A thick paste of AVH (300 mg/20 mL water) was prepared and applied on the shaved skin of rabbits. After 12 h, the skin was observed for redness, rashes and color change.

On the 15th day, blood samples from anesthetized rats were collected in tubes lined with EDTA by cardiac puncture and analyzed for complete blood count, liver function test, renal function test, uric acid, and lipid profile.

### 2.16 Gross necropsy and histopathology of vital organs

After completion of toxicity studies (day 15), all animals were anesthetized and sacrificed. Vital organs, *i.e.*, liver, kidney, heart, intestine, gut, and spleen were removed and preserved in 10% (v/v) formalin. Histopathology studies were performed to investigate the effect of AVH on the architecture of vital organs. Tissues of vital organs were sliced to 4–5 μm thickness with the help of a sharp surgical blade, stained with hematoxylin–eosin dye and evaluated under the microscope (XSZ 107 BN).

### 2.17 Statistical analysis

The results of different parameters of both control and treated groups were recorded as their mean values ± standard deviation (SD). The numeric values of different parameters of the control



group and treated groups of rats were analyzed through the one-way analysis of variance (ANOVA) using Minitab 11 software. One-way ANOVA (Turkey's multi comparison test) was applied using  $P$ -value  $< 0.05$  as statistically significant.

## 3 Results and discussion

### 3.1 Characterization of AVH

*Artemisia vulgaris* hydrogel (AVH) was isolated using the hot water extraction method which appeared as an effective method to get excellent yield (13.68 wt%). Physical properties and micromeritics of AVH account for poor flow-ability due to cohesiveness among particles of AVH (Table S3, ESI†). These results inferred to adopt different granulation methods (*i.e.*, dry or wet granulation) or use of appropriate excipients (granular diluent, glidant, lubricant) when used in tablet formulation. The polysaccharide nature of AVH was determined through different techniques.

Energy dispersive spectroscopy (EDS) analysis (Fig. 1a) indicated that the material is a carbohydrate/polysaccharide due to the presence of carbon and oxygen in the spectrum. EDS image of AVH showed no signs of any other elemental impurity indicating its purity. SEM analysis indicated the rough and groovy surface of the hydrogel in dried powder form (Fig. 1b).

The FTIR spectrum of AVH is depicted in Fig. 1c in which characteristic peaks of  $-OH$  functional groups of mono-saccharide repeating units appear at  $3362\text{ cm}^{-1}$ . The presence of a peak around  $2916\text{ cm}^{-1}$  indicated the  $-CH$  of the saccharide units. Sharp peak present at  $1605\text{ cm}^{-1}$  is indicating the presence  $-C=O$  in AVH polysaccharides.<sup>25</sup> Typical broadband in the FTIR spectrum, which appears for polysaccharides, also appeared in the AVH spectrum between  $1200\text{--}1000\text{ cm}^{-1}$  and a prominent peak height was observed at  $1051\text{ cm}^{-1}$  which was assigned to the glycosidic linkage ( $C-O-C$ ) of polymer chains.<sup>26</sup>

Solid-state CP/MAS  $^{13}\text{C}$  NMR spectrum of AVH (Fig. 1d) showed a typical pyranose sugar pattern of signals and comparable to other polysaccharides.<sup>27</sup> Methyl and carbonyl peaks are assigned in the spectrum indicating the presence of acetylated sugars in AVH. From the above-mentioned structure characterization, it is evident that AVH is a polysaccharide in nature.

Thermogravimetric analysis (TGA) of AVH indicated two-step thermal degradation (Fig. 1e). Decomposition temperatures maxima of both steps were obtained at  $283$  and  $444\text{ }^\circ\text{C}$ , respectively. These high values of the decomposition temperatures and slow rate of decomposition indicated good thermal stability of AVH and comparable to thermal decomposition profile of some other naturally occurring water-swelling polysaccharides, hence defining the polysaccharide nature of AVH.<sup>5,28</sup>

### 3.2 pH-responsive swelling studies of AVH

The swelling behavior of AVH was appraised in deionized water and buffer solutions of pH 1.2, 4.5, 6.8 and 7.4. Minor swelling of AVH in buffers of pH 4.5, 6.8 and 7.4 whereas, in the buffer of pH 1.2, it showed almost off behavior (Fig. 2a) as it is not in ionized form at acidic pH. In the case of the buffer of pH 4.5, 6.8 and 7.4, the carbonyl groups become ionized, originating electrostatic repulsion among polymer chains and higher swelling as well. However, at pH 4.5, less swelling of AVH was observed than pH 6.8 and 7.4 which may be due to the decrease number of ionized carbonyl groups resulting in the less repulsion of ionized moieties. Therefore, the penetration of swelling media, *i.e.*, pH 4.5 buffer, was difficult following in the decreased swelling. The remarkable high swelling capacity of AVH was observed in deionized water (no ions available) due to a lack of charge screening effect in it. It is learned from aforesaid experiments that incredible swelling indices, pH-responsiveness, and rapid swelling make AVH perfect candidate for the development of sustained/controlled/targeted release tablet formulation design for drugs, especially NSAIDs.

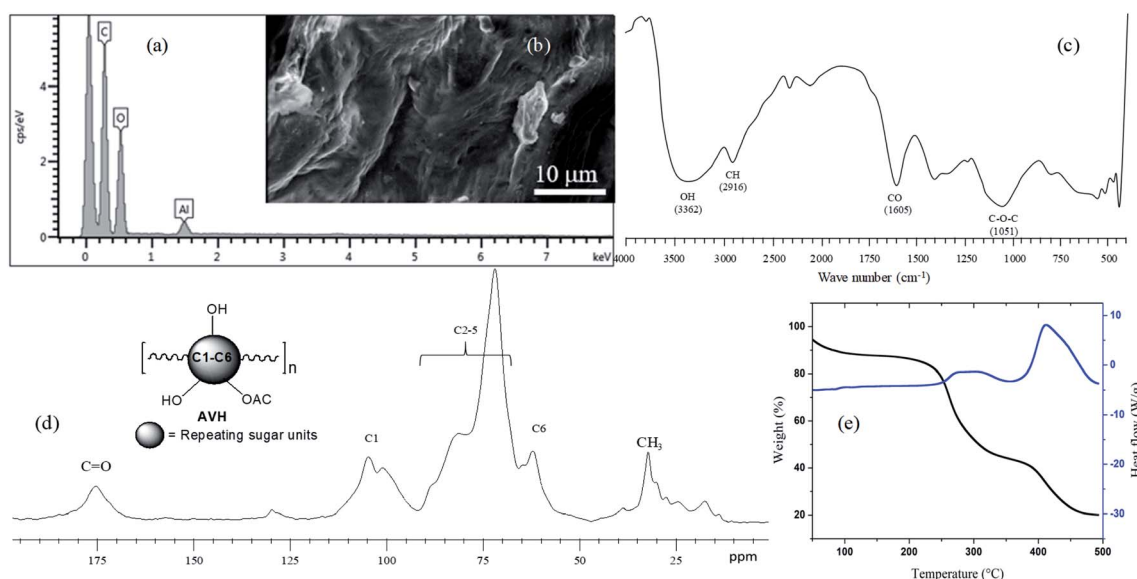


Fig. 1 Characterization of AVH: EDS image (a), SEM image (b), FTIR (KBr) spectrum (c), solid-state CP/MAS  $^{13}\text{C}$  NMR spectrum (d), and TGA and heat flow thermogram (e).



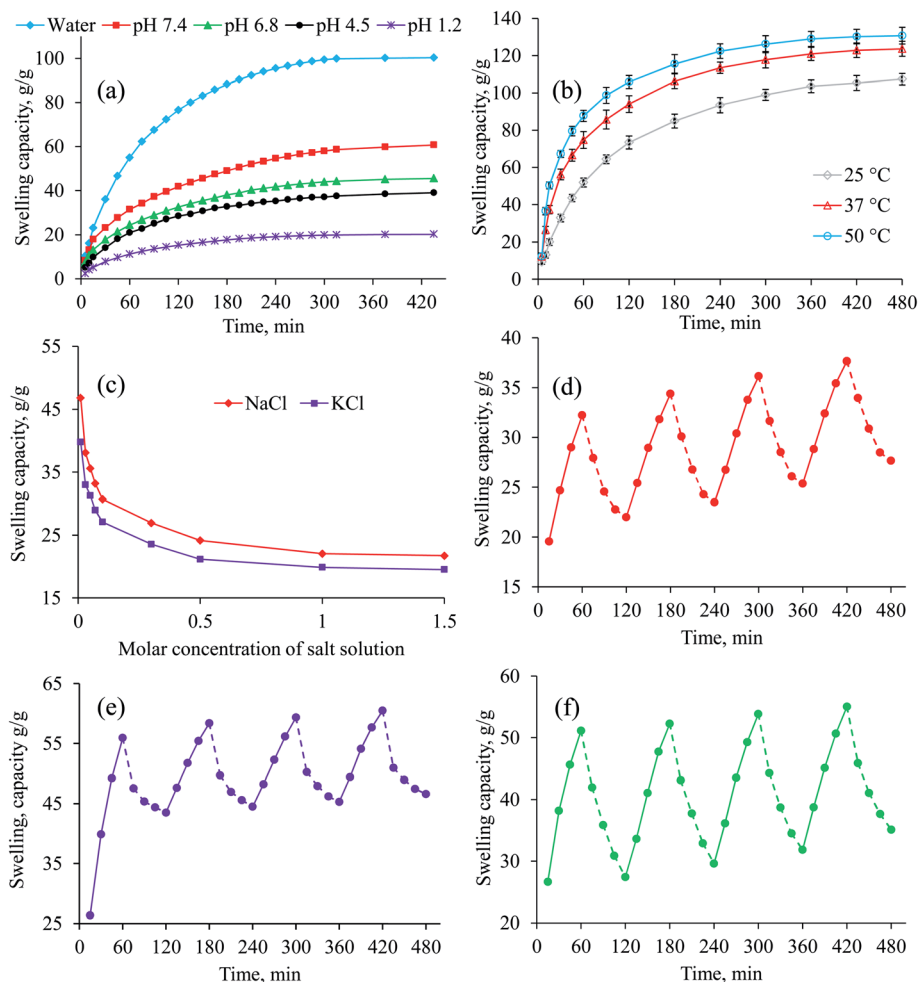


Fig. 2 Swelling studies of AVH at pH 1.2, 4.5, 6.8 and 7.4, and in deionized water (DW) (a), and in DW at 25, 37 and 50 °C (b), equilibrium swelling (after 24 h) of AVH in NaCl and KCl solution (c), and swelling/deswelling of AVH at pH 7.4 and 1.2 (d), in water and normal saline (e) and in water and ethanol (f).

The results of swelling studies of AVH at different temperatures are depicted in Fig. 2b. It was observed that as the temperature of swelling media increased from 25 to 50 °C, the swelling capacity of AVH also increased from 107.3 to 130.6 g g<sup>-1</sup> after 8 h, respectively. At high temperature, due to high kinetic energy of molecules, the polymer chains of AVH were more expanded than at low temperature/less kinetic energy which facilitated the penetration of swelling media. Therefore, swelling capacity of AVH was much higher at high temperature than at low temperature.

### 3.3 Swelling kinetics

The rate of water absorbency by AVH in deionized water and buffer solutions of pH 6.8 and 7.4 showed second-order swelling kinetics (Fig. S1, ESI<sup>†</sup>) indicating its suitability as a material for sustained drug delivery to intestine.<sup>2,17</sup>

### 3.4 Swelling behavior of AVH under electrolyte stress

Equilibrium swelling (after 24 h) of AVH was investigated in salt solutions (NaCl and KCl) of different molar concentrations. The

equilibrium swelling of AVH showed a descending trend with an increase in molar concentrations of electrolytes from 0.01–2 M (Fig. 2c). The abrupt descending trend from 0.01–0.5 M media is due to the charge screening effect of excessive cations present in the swelling media. Additionally, due to the osmotic pressure difference between the salt solution and AVH, the swelling of AVH is decreased as the concentration of salt increases.<sup>29</sup> However, almost similar swelling behavior of AVH was observed from 0.1–2.0 M salt solution. The equilibrium swelling of AVH in NaCl solution was found to be slighter higher than observed in the KCl solution which might be ascribed as less attraction of sodium ions towards its counterions present in AVH than KCl.

### 3.5 Stimuli-responsive on-off switching of AVH

To evaluate pH-responsive swelling/deswelling of AVH, buffers of pH 7.4 and 1.2 were utilized. It was observed that AVH rapidly swells in pH 7.4 while abruptly deswells in pH 1.2. The reason for this swelling/deswelling behavior has been explained earlier in Section 3.2. The on-off switching (4 cycles) experiments of AVH showed reproducible results (Fig. 2d).



AVH shows tremendous swelling in aqueous media and deswells in normal saline solution. The deswelling in normal saline could be accredited to the charge screening effect of additional cations present in the saline solution. Secondly, the osmotic pressure of normal saline is higher than deionized water present in swollen AVH which drained water from swollen AVH resulted in the deswelling of AVH (Fig. 2e).<sup>29,30</sup> A decrease or increase in the osmotic pressure difference between gel and solvent leads to swelling or deswelling, respectively.

There are reports that alcohol can affect drug release behavior from hydrogel-based sustained drug release formulations.<sup>31–33</sup> Therefore, stimuli-responsiveness of AVH in deionized water and ethanol was also probed. Rapid swelling and deswelling of AVH were observed in deionized water and ethanol, respectively attributed to the higher polarity of water (dielectric constant 80.4) and lesser polarity of ethanol. On-off switching cycles in water and ethanol were repeated four times as shown in Fig. 2f and almost the same behavior was observed. It was also observed that during the deswelling phase of AVH at pH 1.2 and in ethanol, AVH did not completely deswell to the initial state. It may be possible that some of the swelling media (pH 7.4 and deionized water) still remain in the AVH powder during the deswelling phase which create hindrance in complete deswelling of AVH.

### 3.6 Scanning electron microscopy of AVH

Swollen then freeze-dried AVH was observed for surface morphology and microporous channeling in it using SEM analysis (Fig. 3). SEM of the transverse view confirmed the uniform distribution of microporous structure with an average of  $55 \pm 30 \mu\text{m}$ . The longitudinal view of AVH exposed the presence of interlinked elongated channels. The excellent swelling of AVH is therefore due to the appearance of such channels which allow rapid absorption of water and other media in it resulting in its high swelling capacity.

### 3.7 *In vitro* and *in vivo* drug release study, and release mechanism

Drug release study from AVH-based tablet formulations (ACF1, ACF2, and ACF3) revealed that ACF release in SGF was only 25.3, 20.6 and 15.8% after 12 h, respectively. Whereas, 98.2% drug was released from ACF1 after 11 h, and 94.2 and 88.2% drug was released from ACF2 and ACF3 after 12 h in SIF, respectively (Fig. 4a). Drug release from ACF1, ACF2, and ACF3 indicated that ACF release in SGF (after 2 h) was 12, 8.72 and 6.34%, respectively. This dwindled drug release in SGF is due to low swelling of AVH in acidic media. However, in the case of SIF, an increase in drug release from tablets was observed owing to the increase in the swelling ability of AVH at near-neutral pH (Fig. 4b). After 12 h, drug release was observed around 97, 90.08 and 82.03% from formulations ACF1, ACF2, and ACF3, respectively. The dissolution study revealed that sustained drug release depends upon increasing the amount of AVH in formulations. Power-law was applied to the underlying drug release mechanism. The  $n$  values were ranging between 0.889–1.064 for all formulations (Table S4, ESI<sup>†</sup>) exhibiting the super case II transport mechanism.<sup>18</sup> The plasma concentration of aceclofenac *versus* time curve is depicted in Fig. 4c. It was observed that the absorption of aceclofenac was delayed from sustained release formulation (ACF1). The value of  $t_{\text{max}}$  was significantly low as compared to ACF1 (8 h) that indicated the enhanced bioavailability of aceclofenac in AVH based formulation which can improve patient compliance. The swelling capacity of tablet formulations after regular time intervals is expressed in Fig. 4d. It was observed that over time, the swelling of tablets increased till 10 h. After that, the erosion of tablets was significantly higher which halted the correct calculation of the swelling capacity of tablets. Furthermore, the swelling capacity of tablets was directly proportional to the concentration of AVH in the formulations. After 10 h, the maximum swelling capacity of ACF1, ACF2 and ACF3 was calculated as 11.03, 11.63 and 13.05  $\text{g g}^{-1}$ , respectively.

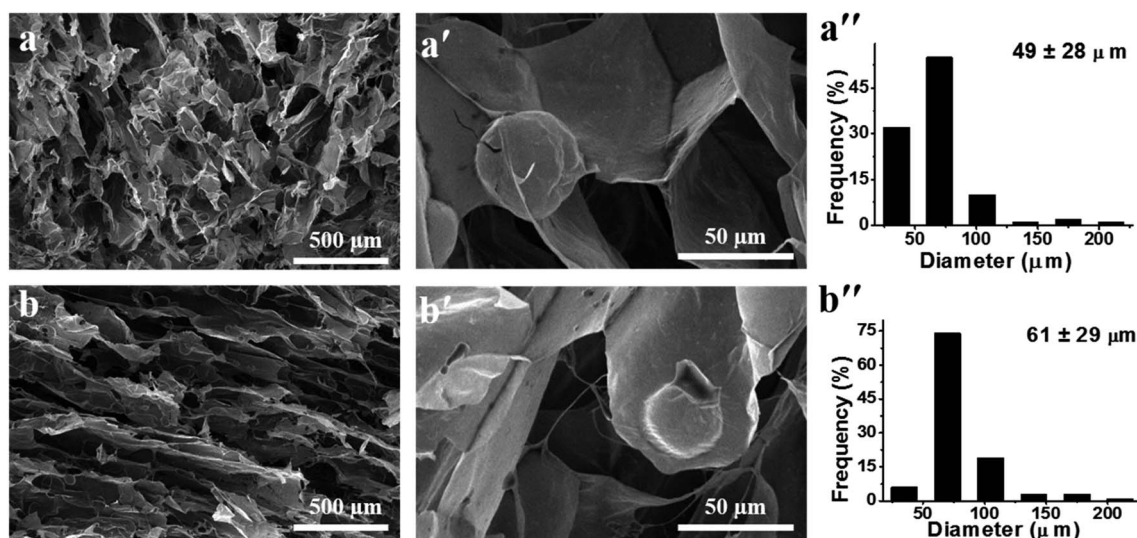


Fig. 3 SEM micrographs of vertical (a and a') and transverse (b and b') cross-sections of freeze-dried AVH respectively, along with their histograms (a'' and b'') (average pore size of  $55 \pm 30 \mu\text{m}$ ).



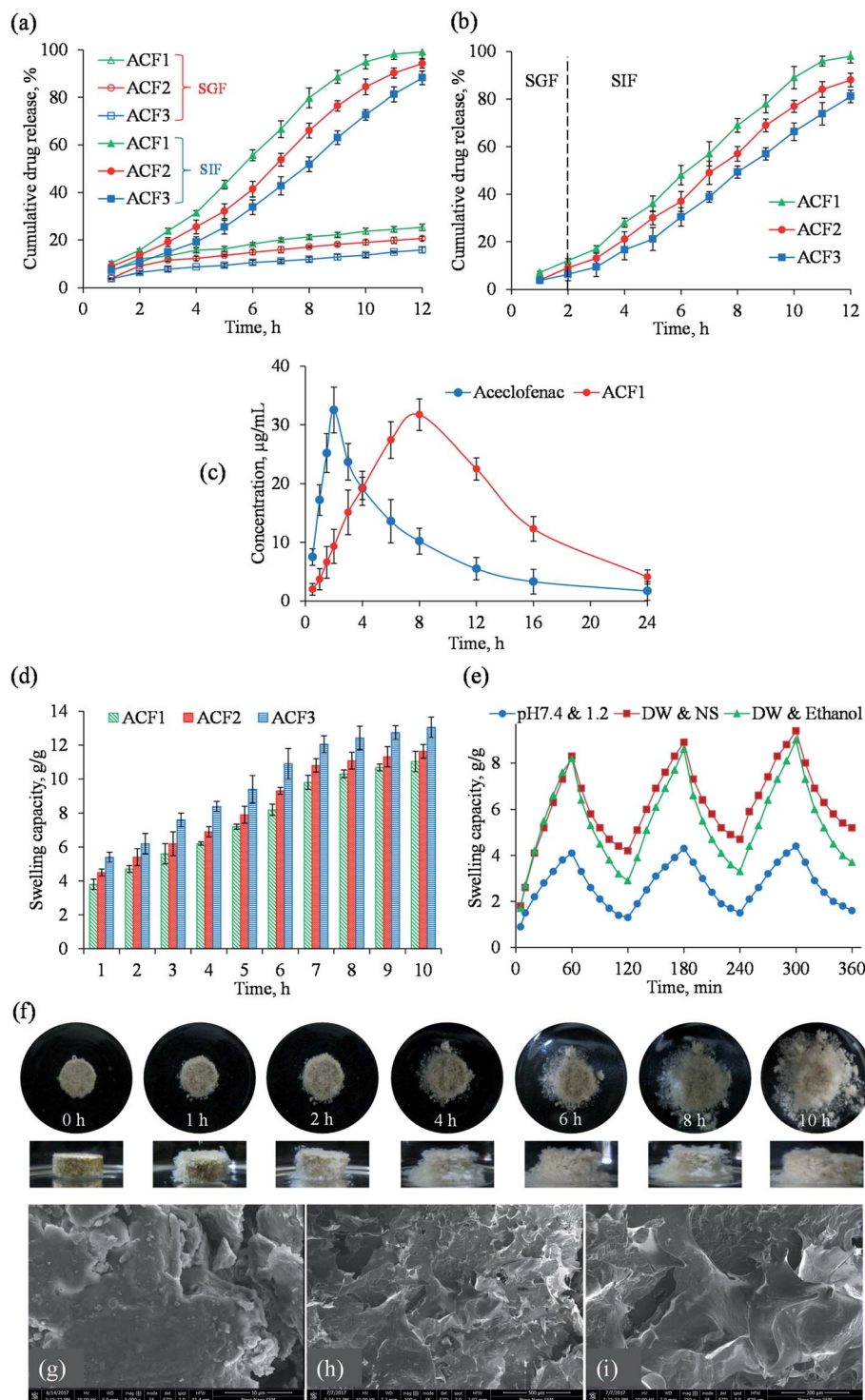
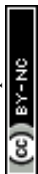


Fig. 4 Aceclofenac release studies from AVH based formulations (ACF1, ACF2, and ACF3) in SGF and SIF for 12 h (a), and in SGF (first 2 h) and SIF (remaining 10 h) (b), pharmacokinetic parameters of ACF1 tablet formulation (c), swelling capacity of three tablet formulations at pH 7.4 after various time intervals (d), stimuli-responsive swelling/deswelling of ACF1 at pH 7.4 and 1.2, in DW and normal saline (NS), and in DW and ethanol (e), radial and axial view of the swelling of AVHF tablet at different time intervals in pH 7.4 buffer (f), and scanning electron micrographs of AVH tablet surface (formulation ACF3) (g) and tablet surface after swelling in water (h and i).

### 3.8 Stimuli responsive swelling studies of AVH tablet formulations

To ascertain the stimuli-responsive swelling/deswelling (on-off switching) of AVH in tablet formulation (ACF1), the buffers of

pH 7.4 and 1.2, deionized water and normal saline, and deionized water and ethanol were used as swelling and deswelling media, respectively. It was observed that even after compression of AVH into tablet form, the swelling and





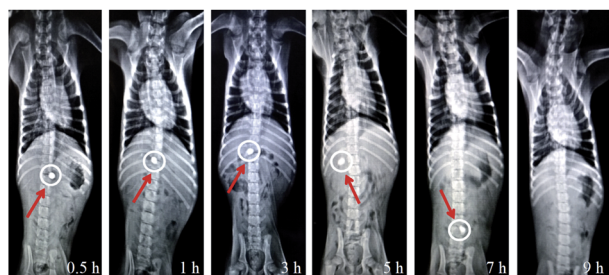


Fig. 5 *In vivo* X-ray photographic images of AVH tablet formulation (AVHF) showing its transit behavior in GIT.

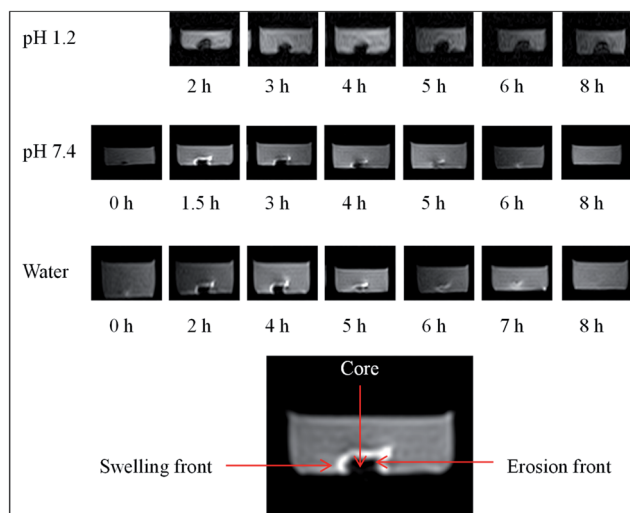


Fig. 6 MRI images of swelling behavior of AVH tablet (AVHM) in water, at pH 1.2 and 7.4 after different time intervals.

deswelling ability of AVH in formulation ACF1 was maintained (Fig. 4e). However, less swelling of AVH in tablet formulation (ACF1) was observed as compared to powder AVH mainly due to decreased in the exposed surface area of AVH in the tablet. Moreover, the interstitial spaces between the particles of AVH in tablet form were decreased (after compression of powdered formulation in the form of tablet) which also contributed to the less swelling of AVH tablet formulation (ACF1).<sup>34,35</sup> Fig. 4f expressed the change in the shape of the ACF3 tablet during the swelling study. SEM images showed a rough and irregular surface of the tablet (ACF3) (Fig. 4g). Once contact with water and as a result of the interaction between hydrophilic groups of AVH and water, the polymeric chains relaxed which resulted in the appearance of pore on the surface of tablets (Fig. 4h and i). These pores further broaden up to initiate the penetration of water in the matrix that is why AVH-based tablet shows channels upon swelling in water.

### 3.9 *In vivo* X-ray study

Radio-graphical images of a stray dog were captured after the ingestion of AVH tablet represented the physical condition of the tablet during transit through GIT. During the 9 h study, it was observed that AVH tablet passed through different

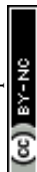
Table 1 Hematological parameters and clinical biochemistry of rats

	Group I	Group II	Group III	Group IV
<b>CBC</b>				
TLC ( $\mu\text{L}^{-1}$ )	8.7	7.9	8.3	9.9
RBC ( $\mu\text{L}^{-1}$ )	6.85	6.7	6.3	6.72
Hb ( $\text{g dL}^{-1}$ )	11.3	12.1	11.4	10.5
HCT (PCV) (%)	38.1	39.4	38.3	37
MCV (fL)	57.3	61.9	60.8	59
MCH (pg)	18.8	19.9	21.9	22
MCHC ( $\text{g dL}^{-1}$ )	28.4	29.5	30.1	32.2
Platelet count ( $\mu\text{L}^{-1}$ )	399	295	347	288
Neutrophils (%)	46	35	29	52
Lymphocytes (%)	51	66	57	61
Monocytes (%)	1	2	2	3
Eosinophils (%)	1	1	1	1
<b>Lipid profile</b>				
Cholesterol ( $\text{mg dL}^{-1}$ )	95	98	107	111
Triglyceride ( $\mu\text{mol L}^{-1}$ )	0.4	0.3	0.4	0.5
HDL ( $\text{mg dL}^{-1}$ )	30	29	33	34
LDL ( $\text{mg dL}^{-1}$ )	33	41	39	46
<b>Liver function test</b>				
Bilirubin ( $\text{mg dL}^{-1}$ )	1.8	0.8	1.3	1.6
SGPT (ALT) ( $\text{IU L}^{-1}$ )	39	33	37	50
SGOT (AST) ( $\text{IU L}^{-1}$ )	96	101	112	124
ALP ( $\text{IU L}^{-1}$ )	102	115	123	100
Total protein ( $\text{g dL}^{-1}$ )	5.0	5.1	5.3	6.0
Albumin ( $\text{g dL}^{-1}$ )	2.0	2.2	2.6	2.6
Globulin ( $\text{g dL}^{-1}$ )	3.0	3.2	3.0	2.5
A/G ratio	0.67	0.69	0.87	1
<b>Renal function test</b>				
Urea ( $\text{mg dL}^{-1}$ )	76	81	78	52
Creatinine ( $\text{mg dL}^{-1}$ )	0.8	0.7	0.9	0.5
<b>Hematology</b>				
ESR ( $\text{mm h}^{-1}$ )	3	2	2.2	2.5
<b>Serum electrolyte</b>				
Potassium ( $\text{mmol L}^{-1}$ )	2.4	2.4	2.6	2.3
Sodium ( $\text{mmol L}^{-1}$ )	135	138	141	143

segments of GIT, *i.e.*, stomach, small intestine, and colon (Fig. 5). A bright and sharp image of the AVH tablet was observed after 0.5 h and 1 h which indicated that the tablet is present almost intact in the stomach of the dog. Images represented after 3 h and 5 h, the size of the tablet was increased whereas the edges of the tablet were soft which indicated the swelling and erosion of the tablet then passed to the colon. After 9 h, the tablet disappeared which indicated the complete disintegration of the tablet in the colon. *In vivo* X-ray studies indicated that AVH containing formulations can be used for small intestine and colon targeted drug delivery systems. Furthermore, AVH can sustain or prolong the release of drugs up to at least 9 h when administered to the animal model.

### 3.10 Swelling/erosion studies of AVH tablet by MRI

In MRI images of AVH tablet in water, pH 1.2 and 7.4 (Fig. 6), the white portion around the tablet indicated the high-intensity



area composed of  $^1\text{H}$  region which is associated with high water ingress, hence, proved the swelling of the tablet.<sup>23</sup> In the black area (core), the intensity of  $^1\text{H}$  region was not observed which indicated the absence of water there. Over time, the swelling media penetrates the tablet resulted in the swelling of the tablet and the increase of distance between the swelling and erosion fronts. This increase in distance can be evident from the increase of the white region (high water intensity area) around the tablet.<sup>36</sup> This MRI study of the tablet showed that the drug release mechanism is depending upon absorption, diffusion and erosion phenomena.

### 3.11 Acute oral toxicity study

All animals were found healthy and active during the 14 days of toxicity studies. No behavioral changes such as tremors, diarrhea, and skin rashes were apparent during 14 days of toxicity studies which demonstrated the non-toxic nature of AVH. Food intake was slightly decreased in treated groups as compared to untreated groups on day 1 after administration of AVH that might be attributed to the fullness of stomach due to intake of AVH (Table S5, ESI<sup>†</sup>). LD<sub>50</sub> of AVH was found to be 7 g per kg body weight in male albino rats which also indicated the safety of AVH. A slight decrease in the mean weight of animals was recorded on day 1–3 which might be attributed to less food consumption on day 1. The loss in weight was recovered gradually. A minor weight gain was recorded in rats from day 9–14 (Table S5, ESI<sup>†</sup>). No significant difference in the amount of food

and water consumed by the treated and untreated animals from day 2 to 14 was observed; however, a statistically significant difference was noticed in food and water consumption in Group II, III and IV animals on day 1 which was normalized as the study progressed. All animals were assigned 0 scores as no signs of iritis and conjunctivitis were observed in any animal after 72 h of instillation of AVH suspension. Eyes of all rabbits were opaque and no redness was noticed after 72 h of administration of AVH suspension indicating the safe excipient for ocular drug delivery system. The overall results demonstrated no sign of irritation, erythema or edema, however, two rabbits of Group IV developed rashes on to the skin. Despite the development of rashes by two rabbits, no other sign of abnormalities was observed in other dermal toxicity parameters. Therefore, these rashes may be considered as accidental. Overall the results demonstrate AVH safe for topical application in different dosage forms, *i.e.*, cream, ointment, lotion, and gel, *etc.* It could be used as a matrix for designing patches for transdermal drug delivery. A comparison of the organ weight of the control group and treated groups of rats reflected no significant difference in the organ weights (Table S6, ESI<sup>†</sup>). All hematological parameters, *i.e.*, RBC, WBC, platelet count, and HBG are in normal ranges and there is no significant difference in the hematological picture of control and treated animals (Table 1). LFT, lipid profile, RFT, and uric acid level were found in normal ranges indicating no signs of toxicity of AVH in treated animals.

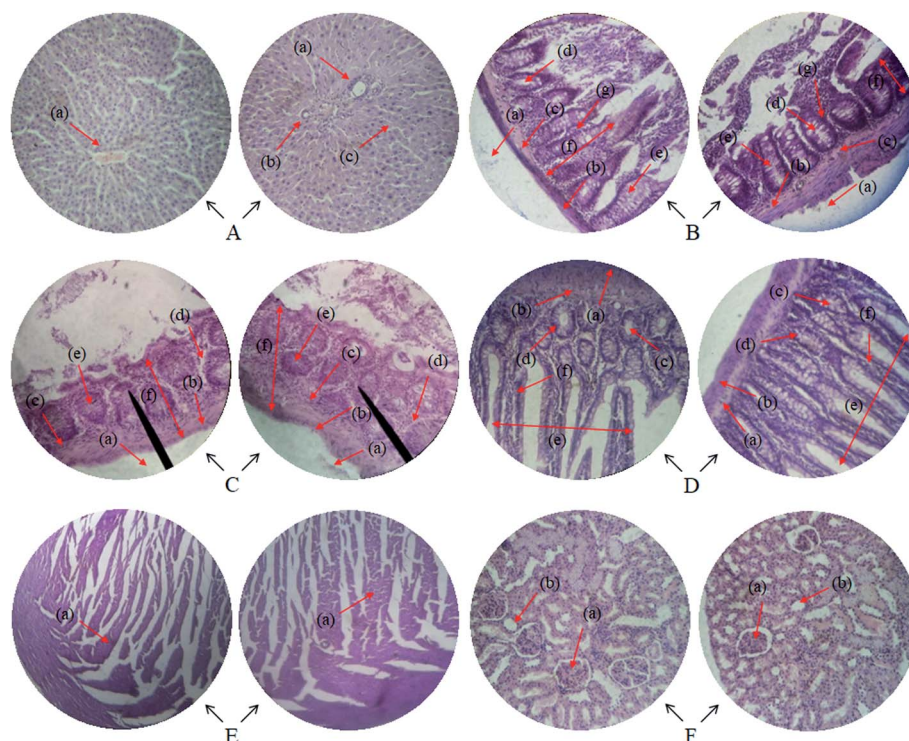


**Fig. 7** Histopathology of liver (A): central vein (a), porta hepatis (b) and plates of hepatocytes (c), colon (B): serosa (a), muscularis externa (b), submucosa (c), lumen of crypt (d), colon crypt (e), mucosa (f) and lamina propria (g), gastric tissues (C): serosa (a), muscularis mucosae (b), submucosa (c), lamina propria (d), gastric glands (e) and mucosa (f), small intestine (D): lamina propria (a), muscularis mucosae (b), acinous lumen (c), columnar epithelial cell with basal nuclei (d), small intestinal villi (e) and small intestinal villus (f), heart (E): striated heart muscles (a) and kidney (F): glomerulus (a) and renal tubules (b).



### 3.12 Gross necropsy and histopathology

The effect of AVH on cellular architecture was evaluated by histopathology studies. The results demonstrated that no changes were noticed in the histological examination of liver, colon, gastric tissues, intestine, heart and kidney of treated rats (Fig. 7). There were no signs of inflammation, necrosis, hemorrhage, and histology of all vital organs.

## 4 Conclusions

*Artemisia vulgaris* hydrogel (AVH) exhibited a remarkably high swelling capacity in the physiological fluids of the body except in pH 1.2 of the stomach. This swelling trend of AVH led to the development of controlled release drug delivery systems (DDS) for ACF which followed the non-Fickian diffusion/super case II transport mechanism. Additionally, the stomach can also be kept safe from hyperacidity caused by ACF due to less swelling of AVH in the stomach environment. Reversible swelling (deionized water and at pH 7.4) and deswelling (ethanol, normal saline and pH 1.2) of AVH can found many applications in the development of intelligent DDS. However, detailed evaluation of AVH as a smart excipient should be carried out before recognized as a pharmaceutical ingredient. *In vivo* swelling behavior of AVH tablet also proved the swelling and erosion of AVH tablet in small intestine and colon. MRI study indicated the swelling of AVH tablet with the passage of time and results are in accord with the tablet behavior in X-ray studies. Pharmacokinetic studies also proved the sustained release behavior of aceclofenac with better pharmacokinetic profile and bioavailability. Eying the outcomes of current acute toxicology studies it could be inferred that AVH is safe as an excipient for oral and topical drug delivery systems. Therefore, AVH appeared a promising smart and natural material for the development of intelligent drug delivery.

## Conflicts of interest

The authors declare no conflict of interest.

## Acknowledgements

We are highly thankful to the Highnoon Research Laboratory (Pvt.) Ltd., Lahore, Pakistan for providing a generous gift of aceclofenac. We also acknowledge the radiology section of the Mubarak Medical Complex, Sargodha, Pakistan for the provision of X-Ray analysis and expert opinion. Manzar MRI, Sargodha, Pakistan is also acknowledged for providing us the facility of analysis. Instruments laboratories, University of Sargodha (UOS) are also being acknowledged for providing us extensive chromatographic and spectroscopic characterization facilities. We are also thankful to Dr Kamran, College of Pharmacy, UOS for helpful discussions regarding pharmaceutical analyses. Photography is the courtesy of one of the authors M. T. Haseeb. We are thankful to M. N. Tahir, KFUPM, KSA for the provision of a solid-state NMR spectrum. Animal houses of The University of Lahore (UOL) and UOS were utilized for animal

hosting and caring, hence we are deeply indebted to both of them. Dr M. Zaman, Faculty of Pharmacy, UOL, Pakistan is also acknowledged for helpful discussion.

## References

- 1 C. I. Abuajah, A. C. Ogbonna and C. M. Osuji, *J. Food Sci. Technol.*, 2015, **52**, 2522–2529.
- 2 M. A. Hussain, G. Muhammad, I. Jantan and S. N. A. Bukhari, *Polym. Rev.*, 2016, **56**, 1–30.
- 3 M. T. Haseeb, M. A. Hussain, S. H. Yuk, S. Bashir and M. Nauman, *Carbohydr. Polym.*, 2016, **136**, 750–756.
- 4 G. Muhammad, M. A. Hussain, M. U. Ashraf, M. T. Haseeb, S. Z. Hussain and I. Hussain, *RSC Adv.*, 2016, **6**, 23310–23317.
- 5 M. S. Iqbal, J. Akbar, M. A. Hussain, S. Saghir and M. Sher, *Carbohydr. Polym.*, 2011, **83**, 1218–1225.
- 6 J. Li and D. J. Mooney, *Nat. Rev. Mater.*, 2016, **1**, 16071.
- 7 P. Matricardi, C. Di Meo, T. Coviello, W. E. Hennink and F. Alhaique, *Adv. Drug Delivery Rev.*, 2013, **65**, 1172–1187.
- 8 G. Leone and R. Barbucci, Polysaccharide based hydrogels for biomedical applications, in *Hydrogels*, Springer, Milano, 2009.
- 9 W. Zhang, X. Zhou, T. Liu, D. Ma and W. Xue, *J. Mater. Chem. B*, 2015, **3**, 2127–2136.
- 10 G. W. Ashley, J. Henise, R. Reid and D. V. Santi, *Proc. Natl. Acad. Sci. U. S. A.*, 2013, **110**, 2318–2323.
- 11 J. K. Oh, D. I. Lee and J. M. Park, *Prog. Polym. Sci.*, 2009, **34**, 1261–1282.
- 12 W. B. Liechty, D. R. Kryscio, B. V. Slaughter and N. A. Peppas, *Annu. Rev. Chem. Biomol. Eng.*, 2010, **1**, 149–173.
- 13 B. A. Lodhi, M. A. Hussain, M. Sher, M. T. Haseeb, M. U. Ashraf, S. Z. Hussain, I. Hussain and S. N. A. Bukhari, *Adv. Polym. Technol.*, 2019, 9583516.
- 14 S. W. Yoon, D. J. Chung and J. H. Kim, *J. Appl. Polym. Sci.*, 2003, **90**, 3741–3746.
- 15 J. Lu, Y. Li, D. Hu, X. Chen, Y. Liu, L. Wang and Y. Zhao, *BioMed Res. Int.*, 2015, 236745.
- 16 A. Kostic, B. Adnadjevic, A. Popovic and J. Jovanovic, *J. Serb. Chem. Soc.*, 2007, **72**, 1139–1153.
- 17 E. Diez-Pena, I. Quijada-Garrido and J. M. Barrales-Rienda, *Macromolecules*, 2002, **35**, 8882–8888.
- 18 P. L. Ritger and N. A. Peppas, *J. Controlled Release*, 1987, **5**, 37–42.
- 19 R. W. Korsmeyer, R. Gurny, E. M. Doelker, P. L. Buri and N. A. Peppas, *Int. J. Pharm.*, 1983, **15**, 25–35.
- 20 K. Abbas, M. A. Hussain, S. N. A. Bukhari, M. Amin and M. Zaman, *J. Drug Delivery Sci. Technol.*, 2019, **52**, 856–862.
- 21 S. H. Patil and G. S. Talele, *Drug Delivery*, 2014, **21**, 118–129.
- 22 S. Baumgartner, J. Kristl, F. Vrecer, P. Vodopivec and B. Zorko, *Int. J. Pharm.*, 2000, **195**, 125–135.
- 23 K. Huanbutta, K. Cheewatanakornkool, K. Terada, J. Nunthanid and P. Sriamornsak, *Carbohydr. Polym.*, 2013, **97**, 26–33.
- 24 J. H. Draize, *J. Pharmacol. Exp. Ther.*, 1944, **82**, 377–390.
- 25 J. C. Boulet, P. Williams and T. Doco, *Carbohydr. Polym.*, 2007, **69**, 79–85.



- 26 M. Kacurakova, P. Capek, V. Sasinkova, N. Wellner and A. Ebringerova, *Carbohydr. Polym.*, 2000, **43**, 195–203.
- 27 B. A. Lodhi, A. Abbas, M. A. Hussain, S. Z. Hussain, M. Sher and I. Hussain, *J. Mol. Liq.*, 2019, **274**, 15–24.
- 28 M. T. Haseeb, M. A. Hussain, S. H. Yuk, M. Amin, S. Bashir and Z. Hussain, *Cellul. Chem. Technol.*, 2018, **52**, 681–688.
- 29 N. A. Peppas and A. G. Mikes, *Hydrogels in Medicine and Pharmacy*, CRC Press, Boca Raton, FL, 1986, vol. 1.
- 30 G. Pass, G. O. Philips and D. J. Wedlock, *Macromolecules*, 1977, **10**, 197–201.
- 31 M. Walden, F. A. Nicholls and K. J. Smith, *Drug Dev. Ind. Pharm.*, 2007, **33**, 1101–1111.
- 32 A. Avachat and D. S. Nandare, *Dissolution Technol.*, 2014, **21**, 11–17.
- 33 V. Friuli, G. Bruni, G. Musitelli, U. Conte and L. Maggi, *J. Pharm. Sci.*, 2018, **107**, 507–511.
- 34 R. S. Harland, A. Gazzaniga, M. E. Sangalli, P. Colombo and N. A. Peppas, *Pharm. Res.*, 1988, **5**, 488–494.
- 35 P. Sriamornsak, N. Thirawong and K. Korkeerd, *Eur. J. Pharm. Biopharm.*, 2007, **66**, 435–450.
- 36 K. Huanbutta, P. Sriamornsak, S. Limmatvapat, M. Luangtana-anan, Y. Yoshihashi, E. Yonemochi, K. Terada and J. Nunthanid, *Eur. J. Pharm. Biopharm.*, 2011, **77**, 320–326.

